Journal of Mineralogical and Petrological Sciences, Volume 104, page 25–36, 2009

Phase relations of nahcolite and trona at high *P-T* conditions

Xi LIU[*,**] and Michael E. FLEET[*]

[*]*Department of Earth Sciences, University of Western Ontario, London, ON N6A 5B7, Canada*
[**]*School of Earth and Space Sciences, Peking University, Beijing 100871, P.R. China*

Using cold-seal hydrothermal bomb and piston-cylinder apparatus, we have carried out both forward and reversal experiments to investigate the phase boundary between nahcolite ($NaHCO_3$) and trona ($NaHCO_3{\cdot}Na_2CO_3{\cdot}2H_2O$). We found that the temperature of this phase boundary remains low at least up to 10 kbar, so that this phase transformation maintains its univariant nature in our investigated *P-T* space. The locus of this phase boundary in a $\log(pCO_2)$–T space is defined as $\log(pCO_2) = 0.0240(\pm0.0001)T - 9.80(\pm0.06)$ (with pCO_2 in bar and T in K), in excellent agreement with earlier 1 atm experiments at different partial pressures of CO_2 (pCO_2) and theoretical calculation. Using this equation and literature thermodynamic data, the entropy of trona at 298.15 K is constrained to be 303.8 J mol^{-1} K^{-1}, essentially identical to earlier estimates from different methods. Our experimental results have also been used to constrain the genesis of nahcolite in some fluid inclusions of diverse origins, and it is suggested that nahcolite in these occurrences is most likely a daughter mineral which crystallized from the fluids as temperature decreased, rather than an accidentally trapped phase.

Keywords: Nahcolite, Trona, Phase relations, Entropy, Fluid inclusions

INTRODUCTION

Nahcolite has a diverse paragenesis. It occurs as massive evaporite ore beds in the Piceance Creek Basin of Colorado (e.g., Dyni, 1996) and the Anpeng deposit in Henan Province of China (e.g., Wang et al., 1991), and as small-sized ore beds, pockets, lenses or concretions in some other geological basins (e.g., Foshag, 1940; Mees et al., 1998; Sugitani et al., 2003). In addition, nahcolite has been reported as a mineral hosted in fluid inclusions in quartz (Larsen et al., 1998; Barrie and Touret, 1999; Bakker and Mamtani, 2000; Ram Mohan and Prasad, 2002) and emerald (Moroz et al., 2001; Vapnik and Moroz, 2002) from metamorphic rocks. Nahcolite is also closely related to carbonatitic volcanoes, where it crystallizes from the orthomagmatic carbonatitic fluids and is preserved within fluid inclusions in quartz and apatite (e.g., Rankin and Le Bas, 1974; Vard and Williams-Jones, 1993; Samson et al., 1995). It occurs also in the alteration products of natrocarbonatitic lavas (e.g., Dawson, 1962; Keller and Krafft, 1990; Zaitsev and Keller, 2006). Moreover, nahcolite has been reported as inclusions in primitive olivine phenocrysts from basaltic magmas of different tectonic environments (Kamenetsky et al., 2001, 2002).

Trona ($NaHCO_3{\cdot}Na_2CO_3{\cdot}2H_2O$) has a similar paragenesis to nahcolite. For example, trona forms evaporite ore beds (e.g., Foshag, 1940), the most well known of which is in the Eocene Green River Formation of Wyoming, occupying an area of over 2000 km^2. Trona also occurs, along with nahcolite, as part of the alteration product of natrocarbonatitic lavas (Keller and Krafft, 1990; Zaitsev and Keller, 2006). And in some cases trona appears to be related to the very final stages of magmatism (Markl and Baumgartner, 2002).

The reaction relating nahcolite to trona is:

$$3NaHCO_3 + H_2O = NaHCO_3{\cdot}Na_2CO_3{\cdot}2H_2O + CO_2 \quad (1),$$

with CO_2 mainly presenting as a vapour phase, and H_2O either as a fluid at low to moderate *P–T* conditions or as part of the vapour at high temperatures (e.g., Duan et al., 1992, 1995). In the three-component system Na_2O–H_2O–CO_2, therefore, this reaction should be univariant in *P–T* space as long as temperature is sufficiently low. Due to the geological importance of nahcolite and trona, this reaction has been determined by experiments performed under different partial pressures of CO_2 (pCO_2) and temperatures at 1 atm (Freeth, 1923; Eugster, 1966). It has also been theoretically calculated for similar conditions

doi:10.2465/jmps.080402
X. Liu, xi.liu@pku.edu.cn Corresponding author
M.E. Fleet, mfleet@uwo.ca

Table 1. Heating experiments with the $NaHCO_3$ reagent starting material in an open air

Heating experiment 1			Heating experiment 2		
T (K)	Time[a] (h)	Mass loss (wt%)	T (K)	Time[a] (h)	Mass loss (wt%)
423	1	8.53	423	1	14.18
423	2	14.41	423	19	36.93
423	3	18.75	423	26	36.93
423	4	21.77	423	43	36.93
423	6	27.55	453	67	36.95
423	8	34.62	473	91	36.96
423	10	36.69	493	139	37.01
423	12	36.93	493	169	37.01
423	24	36.97	513	212	37.01
423	48	36.97	533	380	37.11
423	96	36.97	553	477	37.08
423	192	36.97	573	531	37.09
H_2O content detected: ~ 0.06 wt%			H_2O content detected: ~ 0.19 wt%		

[a] time cumulated from the beginning of heating.

using the ion-interaction model of Pitzer (1973) (Monnin and Schott, 1984). Recently, this phase relation was applied to field observations on some ore deposits (nahcolite ± trona), and it was suggested that there were periods of elevated atmospheric CO_2 content in Earth's history (e.g., Lowe and Tice, 2004; Lowenstein and Demicco, 2006).

Equation (1), however, has never been investigated at elevated pressures. This is surprising, considering the substantial burial depths experienced by those massive ore bodies of nahcolite ± trona and the moderate magmatic/metamorphic pressures recorded by the fluid-inclusion hosts (e.g., 4–8 kbar in Samson et al., 1995; 4 kbar in Barrie and Touret, 1999; 3–7 kbar in Moroz et al., 2001; 3–4 kbar in Vapik and Moroz, 2002; up to 8 kbar in Bakker and Mamtani, 2000). An experimental determination of the reaction between nahcolite and trona at elevated pressures is certainly long overdue.

EXPERIMENTAL DETAILS

Reagent grade $NaHCO_3$ (certified ACS sodium hydrogen carbonate; synthetic nahcolite; Fisher Scientific Company) was used as the starting material for all of our experiments reported here; examination of the starting material with powder X-ray diffraction and FTIR spectroscopy suggested that this material contained no any other additional solid crystalline phase. Although nahcolite absorbs moisture from air, we did not attempt to dry this reagent because $NaHCO_3$ starts to break down at temperatures well below ~ 373 K in an open air (1 atm; e.g., Dei and Guarini, 1997) according to the reaction

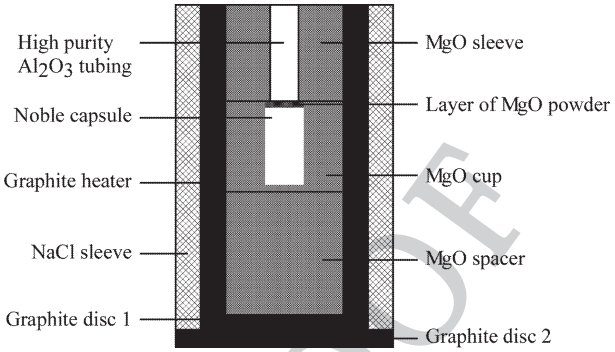

Figure 1. Thick wall assembly used in the piston-cylinder experiments (not to scale). In our laboratory this assembly is usually used to conduct experiments up to 1173 K.

$$2NaHCO_3(s) = Na_2CO_3(s) + H_2O(l) + CO_2(g) \quad (2).$$

In order to monitor the content of free water (molecular water), however, we did heat various amounts of this material to different temperatures at intervals throughout this study and it was found that the content of free water varied from ~ 0.1 to ~ 0.3 wt%, slightly lower than that determined by Hill and Bacon (0.33–0.7 wt%; 1927). The data from two typical heating experiments are shown in Table 1. If the starting material were dry and 100% pure, the theoretical mass loss due to heating at elevated temperatures would be ~ 36.91 wt% [H_2O and CO_2; Equation (2)].

Forward experiments

Forward experiments [from the left side of Equation (1) to the right side] were carried out with a standard cold-seal hydrothermal bomb and a piston-cylinder (Depths of the Earth Company Quickpress). The starting material was loaded into a gold capsule which was immediately sealed by arc-welding. To prevent the breakdown of $NaHCO_3$ during welding, the gold capsule was wrapped in a water-wetted tissue, which might introduce a trace amount of water to the experimental charge.

Experiments with the standard cold-seal hydrothermal bomb were conducted at 0.1, 0.34, 0.69, and 2.07 kbar. A 38.1 mm long gold capsule with the starting material sealed inside was loaded into the Tuttle bomb. Pressure was applied first; and then, temperature was raised to a target value at a rate of 20 K/minute, with pressure carefully maintained. Finally, heating was terminated by switching off the electrical power, and the Tuttle bomb with the experimental capsule in it was quickly cooled in cold water. During the course of an experiment, pressure was carefully monitored and adjusted, and its uncertainty

was estimated to be ~ ±0.02 kbar. Temperature was measured by a Chromel/Alumel thermocouple; the uncertainty in the temperature measurement is ~ ±10 K. For the temperature range covered by our experiments, 15–30 minutes was required for the outside heating furnace and the inner Tuttle bomb to reach their thermal equilibrium.

Experiments with the piston-cylinder apparatus were conducted at 5 and 10 kbar using the 19.05 mm low-friction cell shown in Figure 1 (Mirwald et al., 1975). To further reduce the friction in our experiments, this cell was wrapped in a thin lead foil, and the inner surface of the cylinder was coated with a thin film of molykote. Pressure calibration was done using the melting of dry NaCl at 1323 K (Bohlen, 1984), and the uncertainty in the pressure measurement is ±0.2 kbar. Temperature was measured by either a Chromel/Alumel thermocouple or a WRe_5–WRe_{26} thermocouple, with the effect of pressure on its e.m.f. ignored. In the case of thermocouple failure, temperature was estimated from the settings of the electrical power supply. The tip of the thermocouple was separated from the 8 mm long gold capsule by a 0.5 mm thick layer of MgO powder; it was later found that this thin layer of MgO powder could not effectively prevent the thermocouple tip penetrating into the noble capsule when the experimental pressure reached 10 kbar, so that a harder material like alumina or ruby disc should be used instead. Our experience suggested that the thermocouple reading might be 25 K lower than the real temperature in the hot spot of the graphite furnace, which should be the dominant among the factors affecting the temperature measurement in the piston-cylinder apparatus. Therefore, the uncertainty in the temperature measurement of our piston-cylinder experiments is assumed to be ~ ±25 K. During each experiment, pressure was raised to the target value first, and then temperature was raised using a heating ramp of 150 K/minute. Experiments were terminated and rapidly temperature-quenched by switching off the electrical power supply.

Capsules recovered from our experiments were firstly examined carefully visually. We observed that the capsules from the hydrothermal experiments at relatively low temperatures were generally collapsed whereas those from the hydrothermal experiments at higher temperatures were distended, indicating the absence/presence of a vapour phase. On perforating the distended capsules, vapour escaped quickly and explosively. This phenomenon, however, was not clearly observed for those capsules recovered from the piston-cylinder experiments, presumably due to the much smaller sample sizes and the much higher experimental pressures. Experimental charges were ground under acetone in an agate mortar, and analyzed by powder X-ray diffraction (Rigaku D/MAX-B system; Co*K*α X-radiation). It was found that the visual observations made on the capsules from the hydrothermal experiments (collapsed versus distended) agreed very well with the corresponding X-ray diffraction powder patterns (e.g., compressed capsules yielded nahcolite alone whereas distended capsules contained trona ± nahcolite; see Figure 2 for an example). This agreement led to a convenient method for reversal of Equation (1) using the hydrothermal bomb technique.

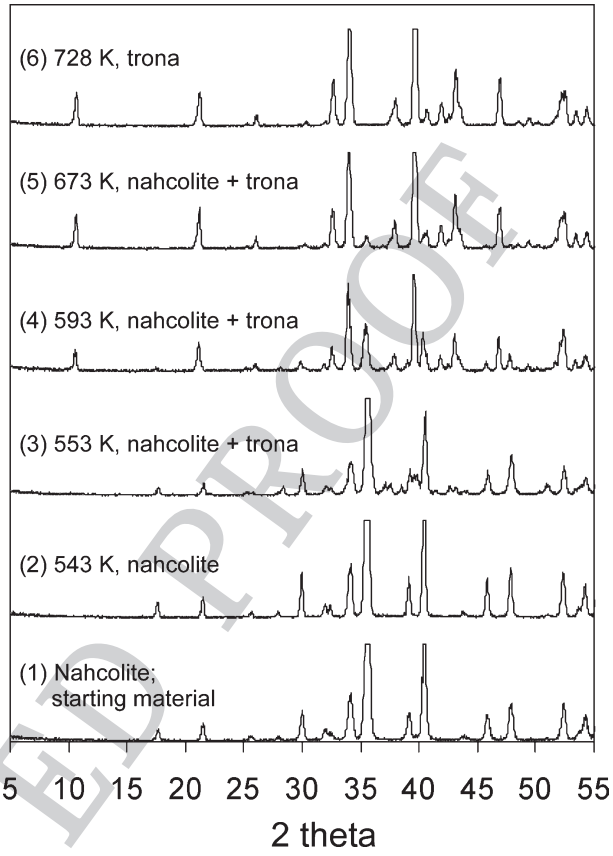

Figure 2. Powder XRD patterns of starting material (nahcolite) and some products of experiments at 2.07 kbar: (1) starting material, nahcolite; (2) LM097, 543 K, compressed capsule, nahcolite only; (3) LM094, 553 K, distended capsule, both nahcolite and trona; (4) LM074, 593 K, distended capsule, both nahcolite and trona; (5) LM059, 673 K, distended capsule, both nahcolite and trona; (6) LM053, 728 K, distended capsule, trona only (Co *K*α X-radiation). Note that only nahcolite was detected by powder XRD in the experimental product from compressed capsules whereas trona ± nahcolite was detected in the experimental product from distended capsules.

Reversal experiments

Reversal experiments were carried out with the hydrothermal bomb only. The experimental procedures for the forward experiments with the hydrothermal bomb were generally followed, except that the experimentation of the

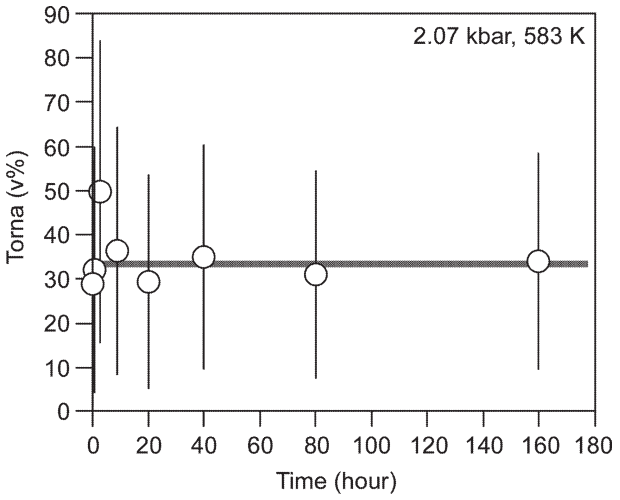

Figure 3. Experiments of different durations at 2.07 kbar and 583 K, showing that the proportion of the product trona is independent of annealing time. The volume proportion of trona to nahcolite was calculated from the X-ray powder diffraction patterns, with the starting material nahcolite and the experimental product trona of LM053 as reference materials. The reflections used in the calculation were 210, 111, 121, and 320 of nahcolite ($NaHCO_3$), and 200, 411 and $\bar{6}04$ of trona.

reversal experiments consisted of two stages. In the first stage, the capsule was heated for a few hours at a temperature slightly above the phase transformation curve (nahcolite + trona + vapour + fluid), which had been already established by the forward experiments. Then the capsule was quenched and carefully checked to assure appropriate swelling. In the second stage, the distended capsule was reloaded in the cold-seal bomb and run at a temperature slightly lower than the transformation value, i.e. in the stability field of nahcolite + fluid, then quenched and opened to confirm the absence of a vapour phase; the absence of trona in the final experimental product was subsequently confirmed by powder XRD. To secure a full reversal, the duration of the second stage of the experimentation was always much longer than that of the first stage.

Evaluation of equilibrium and texture of experimental product

Due to their important commercial value, thermal decomposition studies have been conducted for nahcolite and trona, and a complicated behaviour has been observed (e.g., Caven and Sand, 1911; Gancy, 1963; Templeton, 1978). About 100 years ago, Caven and Sand (1911) found that the dissociation reaction of nahcolite was very slow at temperatures below ~ 363 K (at 1 atm) and noted that encrustation or caking was a serious problem. Gancy (1963), on the other hand, observed the encrustation phenomenon in the case of trona. Presumably due to the same reason, Templeton (1978) observed a metastable phase assemblage with five solid phases [soda ash (Na_2CO_3), trona, wegscheiderite ($Na_2CO_3 \cdot 3NaHCO_3$), thermonatrite ($Na_2CO_3 \cdot H_2O$), and nahcolite] when he studied the thermal decomposition of nahcolite in a closed experimental apparatus at 533 K with variable confining pressure. In contrast, phase equilibrium studies in the system Na_2O-H_2O-CO_2 have shown that a close approach to phase equilibrium is easily and quickly achieved (e.g., Hill and Bacon, 1927; Waldeck et al., 1934; Eugster, 1966). Indeed, the relatively rapid reactions in this system are exploited in the processing of soda ash ores.

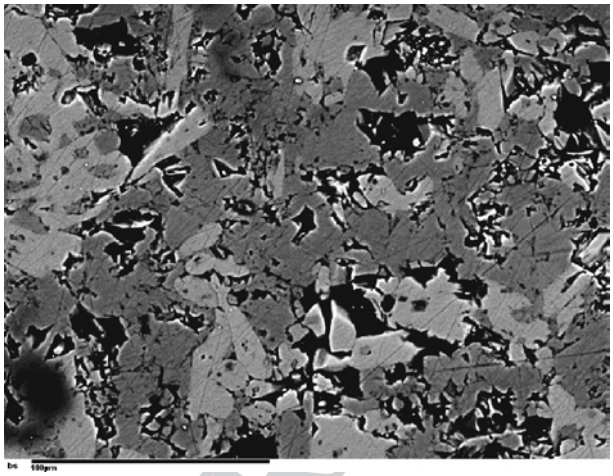

Figure 4. BSE image showing the texture of the experimental product of LM063 (0.69 kbar, 523 K). Bright grains are nahcolite while grey grains trona. No apparent encrustation of nahcolite by trona was observed in this study.

In this study, eight hydrothermal experiments with durations ranging from 0 to 160 hours were performed at 2.07 kbar and 583 K to evaluate the state of equilibrium of our experiments (Table 2). As expected, the phases in the products are nahcolite, trona and vapour (see later discussion). The phase proportion extracted from the powder X-ray diffraction data shown in Figure 3 is largely independent of run duration, implying that the forward reaction is almost instantaneous.

Additionally, some of our experimental products were checked by using electron microprobe (JEOL JXA-8600) back-scattered (BSE) images, and no apparent encrustation of nahcolite by trona was found. Fig. 4 shows the typical texture of the experimental products. Our favoured explanation for the nominal discrepancy between the phase equilibrium and thermal decomposition studies (no encrustation *versus* encrustation) is that the experimental pressure in the former was fixed while it evolved naturally in the latter.

In summary, we believe that the present experiments

Table 2. A time study at 2.07 kbar and 583 K with the hydrothermal reaction vessel

Run #	Time (h)	Observation	Trona (v%)[a]
LM124	0	nahcolite + trona + vapour[b]	29(28)[c]
LM123	0.5	nahcolite + trona + vapour	32(28)
LM122	2.5	nahcolite + trona + vapour	50(34)
LM125	9	nahcolite + trona + vapour	36(28)
LM095	20	nahcolite + trona + vapour	29(28)
LM099	40	nahcolite + trona + vapour	35(26)
LM100	80	nahcolite + trona + vapour	31(24)
LM126	160	nahcolite + trona + vapour	34(25)

[a] Proportion of trona in experimental product (by volume%) was calculated from X-ray data, with any vapour or fluid ignored.
[b] Presence of vapour demonstrated by distended capsule and explosive release of gas.
[c] Average followed by one standard deviation, read as 29 ± 28.

were conducted under either equilibrium conditions or conditions closely approaching equilibrium.

EXPERIMENTAL RESULTS

Table 2 summarizes the experiments at 2.07 kbar and 583 K which have been used to evaluate the equilibrium state of our experiments, Table 3 the forward experiments conducted at 0.1, 0.34, 0.69, and 2.07 kbar with the hydrothermal bomb, Table 4 the forward experiments conducted at 5 and 10 kbar with the piston-cylinder apparatus, and Table 5 the reversal experiments conducted at 0.34, 0.69 and 2.07 kbar with the hydrothermal bomb. In total, 51 hydrothermal experiments and 8 piston-cylinder experiments were carried out from 0.1 to 10 kbar and 328 to 848 K. In these experiments, the observed phases are nahcolite, trona, fluid and vapour. Figs 5 and 6 show the experimental results, with the major experimental finding as that the phase transformation temperature between nahcolite and trona is very low (See later discussion).

X-ray diffraction powder patterns for the various experimental products indicated that the solid crystalline phases in the experimental products were nahcolite and trona only (see Fig. 2 for some examples). The patterns of the single phase products closely corresponded to the JCPDS reference patterns, and were very closely reproduced by calculation using program POWDER2 (Pennsylvania State University) and literature crystal structure data. It is therefore assumed that these solid phases were most likely stoichiometric.

The exact nature of the fluid and vapour in the present experiments is not very clear; this, however, does not influence our results reported here. The room pressure experiments of Eugster (1966) were performed at 293-343 K in the presence of excess aqueous solution, with the

Table 3. Experiments with the hydrothermal reaction vessel

Run #	T (K)	Time (h)	Observation	Trona (v%)[a]
Experiments at 0.1 kbar[b]				
LM105	453	24	nahcolite + fluid[c]	
LM107	463	24	nahcolite + fluid	
LM108	493	24	nahcolite + fluid	
LM106	503	24	nahcolite + fluid	
LM113[d]	513	24	nahcolite + trona + vapour	
LM114[d]	548	24	nahcolite + trona + vapour	
Experiments at 0.34 kbar				
LM112	493	24	nahcolite + fluid	
LM111	503	24	nahcolite + fluid	
LM116	513	24	nahcolite + trona + vapour	
LM115	523	24	nahcolite + trona + vapour	
Experiments at 0.69 kbar				
LM035	328	90	nahcolite + fluid	
LM036	338	90	nahcolite + fluid	
LM037	353	27	nahcolite + fluid	
LM045	448	24	nahcolite + fluid	
LM047	493	24	nahcolite + fluid	
LM050	508	24	nahcolite + fluid	1(2)[e]
LM060	523	24	nahcolite + fluid	7(7)
LM063	523	24	nahcolite + trona + vapour	37(8)
LM061	533	24	nahcolite + trona + vapour	44(7)
LM062	538	24	nahcolite + trona + vapour	37(6)
LM049	548	24	trona + vapour	99(1)
LM048	568	24	trona + vapour	
LM046	568	24	trona + vapour	
Experiments at 2.07 kbar				
LM043	383	72	nahcolite + fluid	
LM042	418	24	nahcolite + fluid	
LM041	428	86	nahcolite + fluid	
LM096	533	20	nahcolite + fluid	
LM097	543	20	nahcolite + fluid	1(2)
LM098	553	80	nahcolite + fluid	
LM094	553	20	nahcolite + trona + vapour	22(22)
LM095	583	20	nahcolite + trona + vapour	29(28)
LM074	593	20	nahcolite + trona + vapour	71(8)
LM051	633	24	nahcolite + trona + vapour	90(8)
LM065	643	24	nahcolite + trona + vapour	81(10)
LM064	653	24	nahcolite + trona + vapour	92(4)
LM059	673	24	nahcolite + trona + vapour	93(5)
LM057	683	24	nahcolite + trona + vapour	97(3)
LM056	708	24	nahcolite + trona + vapour	84(7)
LM053	728	24	trona + vapour	98(4)
LM054	848	24	trona + vapour	

[a] It was calculated from X-ray data, with any vapour or fluid ignored.
[b] Experiments at 0.1 kbar might suffer serious problem in pressure measurement.
[c] A fluid phase was required by mass-balance; it was not directly observed.
[d] During quenching capsule was exploded, with the experimental charge gone.
[e] Average followed by one standard deviation, read as 1 ± 2.

Table 4. Experiments with the piston–cylinder apparatus

Run #	T[a] (K)	Time (h)	Observation	Trona (v%)[b]
Experiments at 5 kbar				
LM103	548	20	nahcolite + fluid[c]	4(5)[d]
LM071[e]	583	18	nahcolite + trona + vapour	23(7)
LM072	603	15	nahcolite + trona + vapour	42(8)
LM070[e]	643	17.5	nahcolite + trona + vapour	72(3)
LM073	718	16	nahcolite + trona + vapour	78(4)
LM069[e]	758	10.5	nahcolite + trona + vapour	79(3)
Experiments at 10 kbar				
LM090	648	12	nahcolite + trona + vapour	
LM091	698	10	nahcolite + trona + vapour	

[a] Correction was made to account for the temperature gradient in the high pressure cell.
[b] It was calculated from X-ray data, with vapour and fluid ignored.
[c] A fluid phase was required by mass-balance; it was not directly observed.
[d] Average followed by one standard deviation, read as 4 ± 5.
[e] Thermocouple failed, and temperature was estimated by electrical power supply.

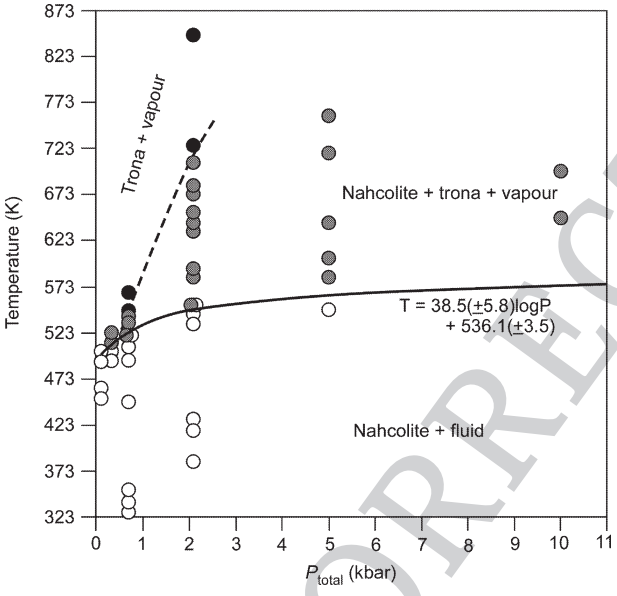

Figure 5. *P–T* phase diagram defined by the forward experiments related to Equation (1): empty symbols are the experiments showing the phase assemblage of nahcolite + fluid while filled symbols are the experiments showing the phase assemblage of trona + vapour ± nahcolite (filled symbols in dark, trona + vapour; filled symbols in grey, nahcolite + trona + vapour). The complete transformation from nahcolite to trona demonstrated by the experiments at relatively high temperatures at 0.69 and 2.07 kbar might indicate another phase transformation, as shown by the broken curve.

identities of solution (fluid) and vapour well established. For high *P–T* conditions, however, there are insufficient experimental and theoretical data available to accurately describe the state of H_2O as fluid or vapour: there are extensive literature data for the CO_2–H_2O, CH_4–CO_2–H_2O and NaCl–H_2O–CO_2 systems above 1 bar (e.g., Sterner and Bodnar, 1991; Duan et al., 1992, 1995), but not for the present Na_2O–CO_2–H_2O system. Thanks to the major experimental result found in this investigation, the transformation of nahcoltie to trona [Equation (1)] taking place at very low temperatures (Tables 3, 4 and 5), the identities of fluid and vapour can be positively determined theoretically, as outlined below.

Table 5. Reversal experiments with the hydrothermal reaction vessel

Run #	P (kbar)	T (K)	Time (h)	Observation
LM117	0.34	518	4	Distended capsule (vapour)
		508	18	Distended capsule (vapour)
LM119	0.34	518	4	Distended capsule (vapour)
		498	24	Compressed capsule (no vapour)
LM068	0.69	531	24	Distended capsule (vapour)
		522	48	Compressed capsule (no vapour)
LM121	2.07	553	2	Distended capsule (vapour)
		543	24	Compressed capsule (no vapour)

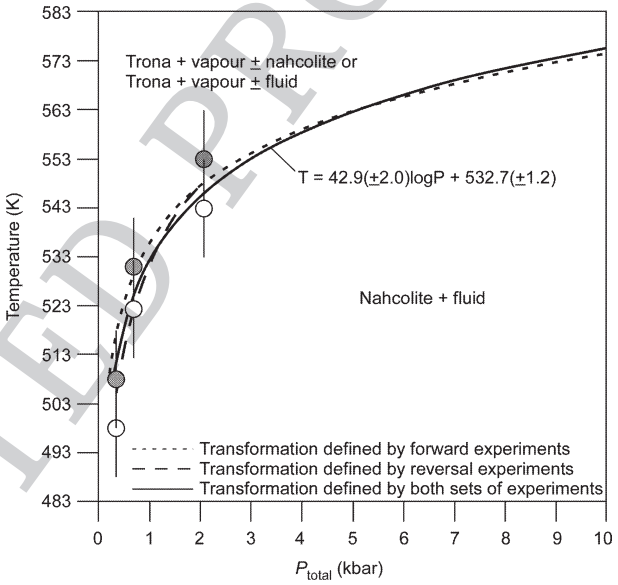

Figure 6. Univariant *P–T* curve for Equation (1) defined by both forward and reversal experiments.

Phase assemblage at low temperatures and univariant nature of Equation (1)

Since the starting material in our experiments is nahcolite plus a small amount of free water (from the air or the water-wetted tissue), the stable phase assemblage at temperatures lower than the transformation temperature should be nahcolite + fluid, as required by the low temperatures and the mass-balance consideration (Figs. 5 and 6).

The P–T condition of the critical point of pure H_2O is well known as 0.218 kbar and 647.3 K. With the introduction of nahcolite, the fluid phase should dissolve some $NaHCO_3$ in it; because the amount of free water in the experimental charge was very low, however, the most of the nominal nahcolite content should have maintained its identity as a solid phase in our experiments at low temperatures (Hill and Bacon, 1927; Waldeck et al., 1934). Although there has not been any experimental measurement on the solubility of $NaHCO_3$ in water at high pressures or experimental study on the effect of $NaHCO_3$ on the P–T of the critical point, it is probable, by analogy to the $NaCl$–H_2O–CO_2 system, that $NaHCO_3$ will not affect the critical temperature of water substantially; if there is any salting effect, it should increase the critical temperature and thus enlarge the stability field of the fluid (Hendel and Hollister, 1981). Consequently, water must be present as a fluid phase in the experiments at temperatures lower than the transformation temperature; e.g. at 10 kbar, the temperature to initiate Equation (1) is ~ 575 K (Figs. 5 and 6), which is much lower than the critical temperature of pure water. This is very important, because it confirms that Equation (1) should be univariant at pressures up to at least 10 kbar.

Transformation of nahcolite/trona and evolution of pCO_2

When temperature reaches the phase transformation temperature, Equation (1) will start to take place, trona and CO_2 (vapour) be produced at the expense of nahcolite and water (fluid), and some H_2O partition into the vapour phase (e.g., Sterner and Bodnar, 1991; Duan et al., 1992). As the reaction progresses towards its equilibrium, the volume of the vapour phase increases, so that pCO_2 increases from ambient to some unknown value which might be slightly lower than P_{total} due to the minor contribution of H_2O in the vapour. When the final equilibrium is attained, the final phase assemblage along the univariant curve should be nahcolite + trona + fluid (H_2O-rich) + vapour (CO_2-rich), with pCO_2 approximating P_{total} because of the very small quantity of water in the experimental charge. Once the temperature raises further and the system moves away from the univariant curve, water, whether it is in the fluid phase or vapour phase, will be immediately eliminated from the system due to the formation of trona (See later discussion), so that pCO_2 should become strictly equal to P_{total}.

The forward experiments are shown in Figure 5. At low temperatures the divariant phase assemblage of nahcolite + fluid is stable up to at least 10 kbar, in agreement with Kagi et al. (2005). The univariant nahcolite/trona phase boundary is defined by the first appearance of trona on heating the nahcolite starting material to a temperature given by $T = 38.5(\pm5.8)\log P + 536.1(\pm3.5)$ with P in kbar and T in K (Fig. 5). The reversal experiments, plus the univariant curve of nahcolite + trona + vapour + fluid derived in Figure 5, are plotted in Figure 6. The univariant nahcolite/trona phase boundary is defined by the first disappearance of vapour in the reversal experiments. Clearly the reversal experiments define a P–T locus for Equation (1) which is generally about 5 to 10 degrees lower than that constrained by the forward experiments. This discrepancy is essentially within the accuracy of the temperature measurement in our experiments. Finally, the curve for the equilibrium phase boundary was fitted to the median of the two sets of experimental points (from the forward and reversal experiments), giving $T = 42.9(\pm2.0)\log P + 532.7(\pm1.2)$, with P in kbar and T in K.

Divariant field of nahcolite + trona + vapour

When temperature increases above the transformation value, one phase will be eliminated and the system becomes divariant. In Eugster's (1966) experiments the phase to be eliminated apparently was nahcolite because the solution (H_2O-rich fluid) was in excess; in contrast, the most likely phase to be eliminated in our experiments is the fluid phase due to the very low content of H_2O in the experimental charge, so that the stable phase assemblage after the phase transition should be nahcolite + trona + vapour, as revealed by our visual observation and X-ray diffraction data (Tables 2, 3 and 4).

A few experiments demonstrating the phase assemblage of trona + vapour were observed at relatively high temperatures at 0.69 and 2.07 kbar (Fig. 5), which potentially implies another phase transformation. Its mechanism is currently under experimental investigation.

DISCUSSION

Nahcolite/trona phase relations

The phase relations of nahcolite and trona coexisting with a fluid phase (H_2O-rich) and a vapour phase (CO_2-rich) were previously studied at room pressure by Freeth (1923) and Eugster (1966), who carried out experiments at 1 atm with different pCO_2, and Monnin and Schott (1984), who calculated the 1 atm phase diagram using the ion-interaction model of Pitzer (1973). These earlier studies are compared with the present investigation in a plot of $\log(pCO_2)$ versus T (Fig. 7). Note that in plotting the present results on Figure 7, we have assumed $pCO_2 \approx P_{total}$ along the univariant curve, as previously discussed. Mon-

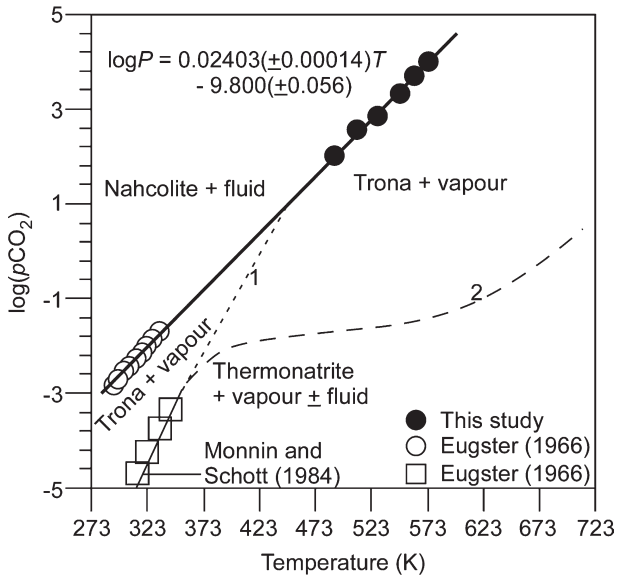

Figure 7. Phase relations of nahcolite, trona and thermonatrite ($Na_2CO_3·H_2O$) in log(pCO_2)–T space (pCO_2 in bars and T in K). For the equilibrium of nahcolite and trona, the data points of this study are from the equation in Fig. 6 while those of Eugster (1966) are from his experiments. Note the excellent agreement for the nahcolite/trona equilibrium [Equation (1)] between this study at high pressure and the literature studies at P_{total} = 1 atm. For the equilibrium of trona and thermonatrite [Equation (6)], the data points of Eugster (1966) are from his experiments, and the result of Monnin and Schott (1984) which is shown as a short curve is from their theoretical calculation.

nin and Schott (1984) pointed out that their calculations and Eugster's (1966) experiments on the location of the nahcolite/trona boundary at P_{total} = 1 atm were in very good agreement. Figure 7 now shows that our experimental data at high pressures are in very good agreement with these two earlier studies at room pressure. We conclude that the nahcolite/trona phase boundary extends almost linearly in the log(pCO_2)–T space to at least 10 kbar ($pCO_2 \approx P_{total}$): the linear regression equation for the phase boundary is $\log(pCO_2) = 0.02403(\pm0.00014)T - 9.800(\pm0.056)$.

Entropy of trona at 298.15 K

No calorimetric measurements have been made on trona. Vanderzee (1982), using limited phase equilibrium data at room pressure and some assumptions, tentatively suggested that the entropy of trona at 298.15 K is ~ 303.13 ± 1.7 J mol^{-1} K^{-1}, which agreed well with the estimate made by Rupert et al. (1965; 302.9 J mol^{-1} K^{-1}). Due to some unknown reasons, these values however were not included in the major compilations of thermodynamic data such as Robie and Hemingway (1995). Our well defined nahcolite/trona phase transformation can be used to further constrain the entropy of trona at 298.15 K.

The general condition for the thermodynamic equilibrium of the phase transformation of nahcolite and trona [Equation (1)] can be expressed as:

$$\Delta G(P,T) = \Delta G(1,T) + \int_1^P \Delta V(P,T)dP + RT\ln K = 0 \quad (3),$$

where $\Delta G(P,T)$ is the Gibbs free energy change for the reaction among pure end members at the pressure and temperature of interest, $\Delta G(1,T)$ the Gibbs free energy change for the reaction among pure end members at 1 bar and the temperature of interest, $\Delta V(P,T)$ the volume change for the reaction among the pure end members at the pressure and temperature of interest, P pressure, R gas constant (8.3143 J K^{-1} mol^{-1}), T temperature and

$$K = \frac{[\alpha^{Trona}_{Na_2CO_3.NaHCO_3.2H_2O}][\alpha^{Vapour}_{CO_2}]}{[\alpha^{Nahcolite}_{NaHCO_3}]^3[\alpha^{Fluid}_{H_2O}]} \quad (4).$$

Our powder XRD data suggested that nahcolite and trona are most likely pure solid phases. In addition, we assume the fluid phase consists of 100% water, neglecting any dissolution of $NaHCO_3$ and $Na_2CO_3·NaHCO_3·2H_2O$ at 298.13 K (Waldeck et al., 1934). According to the literature experimental measurements (e.g., Wiebe and Gaddy, 1939) and thermodynamic modeling (e.g., Duan et al., 1992, 1995; Duan and Sun, 2003), the abundance of CO_2 in this fluid at the transformation condition of 298.15 K and 0.00229 bar should be negligible (Fig. 5). Furthermore, the supercritical CO_2–rich vapour phase at the phase transformation can be treated as a pure phase because the solubility of H_2O should be very low (e.g., Chrastil, 1982; Duan et al., 1992, 1995; Duan and Sun, 2003). Consequently K is approximately 1, and the term $RT\ln K$ is negligible.

Replacing $\Delta G(1,T)$ by the entropy and the enthalpy terms, and choosing P = 0.00229 bar and T = 298.15 K as the transition point of interest (Fig. 7), we then recast Equation (3) into:

$$\Delta G(P,T) = \Delta H(1,T) - T\Delta S(1,T) + \int_1^P \Delta V(P,T)dP = 0 \quad (5),$$

where $\Delta H(1,T)$ and $\Delta S(1,T)$ are, respectively, the enthalpy change and entropy change for the reaction at 1 bar and 298.15 K. Since most physical data are not available for the phases involved here, we have to assume that the volume changes of nahcolite, trona and fluid (H_2O–rich) are negligible. This is a very reasonable assumption because

Table 6. Thermodynamic data used in estimating the entropy of trona at 298.15 K

	H_0 (kJ mol^{-1})	S_0 (J mol^{-1} K^{-1})	V_0 (cm^3 mol^{-1})
Nahcolite	-949	102.1	38.08
H_2O (fluid)	-285.8	70	18.07
Trona	-2682.1	**303.8**	107
CO_2 (vapour)	-393.5	213.8	24789.7
Thermonatrite	-1429.7	168.1	54.99

All data except the entropy of trona are from Robie and Hemingway (1995).

there is a vapour phase (CO_2-rich) in the study system. Further, the vapour phase (CO_2-rich) can be handled as an ideal gas because the transition pressure (0.00229 bar) at 298.15 K is extremely low. We must emphasize here that only the thermodynamic data at 298 K are needed for this calculation, and that the whole process is essentially an isothermal expansion process of an ideal gas.

With the thermodynamic data listed in Table 6, Equation (5) gives the entropy of trona at 298.15 K as 303.8 J mol^{-1} K^{-1}, which is essentially identical to the estimates of Vanderzee (1982; 303.13 ± 1.7 J mol^{-1} K^{-1}) and Rupert et al. (1969; 302.9 J mol^{-1} K^{-1}).

Transformation pressure of trona/thermonatrite at 298.15 K

The transformation reaction between trona and thermonatrite ($Na_2CO_3 \cdot H_2O$) is:

$$2NaHCO_3 \cdot Na_2CO_3 \cdot 2H_2O = 3Na_2CO_3 \cdot H_2O + 2H_2O + CO_2 \quad (6),$$

in which H_2O is present as a fluid phase and CO_2 as a vapour phase as long as temperature is not too high. In this case, this reaction is univariant (Fig. 7). At elevated *P*–*T* conditions, however, H_2O and CO_2 should mix completely to form one single vapour phase (e.g., Duan et al., 1992, 1995), so that the reaction is not univariant any more and the phase relations should change dramatically.

Equation (6) at low *P*–*T* conditions has been experimentally investigated by Eugster (1966) and theoretically calculated with the ion-interaction model of Pitzer (1973) by Monnin and Schott (1984), and has been found to be univariant indeed. According to these two studies, the trona/thermonatrite transformation [Equation (6)] only occurs at very low pCO_2 when temperature is low (e.g., $pCO_2 \approx$ 10–20 ppm at 1 bar total pressure and ~ 313.15 K). However, it has been pointed out that pCO_2 values as low as this could not have been measured accurately in these early experiments (Vanderzee, 1982; Monnin and Schott, 1984).

The entropy of trona at 298.15 K derived in the last section, along with other thermodynamic data in the literature (Table 6), can be tentatively used to constrain the transformation pressure of trona and thermonatrite at 298.15 K. This is a constructive exercise, although trona might not coexist with thermonatrite + fluid (H_2O-rich) + vapour (CO_2-rich) at this temperature (Eugster, 1966; Monnin and Schott, 1984). The similarity of Equations (1) and (6) argues that, essentially, we can treat the phase transformation of trona and thermonatrite in the same way as the phase transformation of nahcolite and trona. Our calculation suggests that the transformation pressure at 298.15 K should be ~ 0.0000007 bar; i.e., pCO_2 = 0.7 ppm at 1 bar total pressure, much lower than the values suggested by Eugster (pCO_2 < 20 ppm; 1966) and Monnin and Schott (pCO_2 < 10 ppm; 1984). Clearly a large discrepancy still exists for the phase transformation of trona and thermonatrite at low *P*–*T* conditions.

To date there is little information on the phase transformation of trona to thermonatrite at elevated *P*–*T* conditions. If the results for the equilibrium of trona and thermonatrite at low *P*–*T* conditions from Eugster (1966) and Monnin and Schott (1984) are linearly extrapolated to high *P*–*T* conditions (curve 1 in Fig. 7), one obtains a very limited stability field for trona. As we previously discussed, Equation (6) does not appear to be univariant under high *P*–*T* conditions, so that the linear extrapolation must be problematic. Indeed, the linear extrapolation apparently contradicts our experimental observation that trona is stable to much higher *P*–*T* conditions (Tables 2, 3 and 4). The equilibrium curve of trona and thermonatrite probably shifts to much higher temperatures as pressure increases, as tentatively suggested by curve 2 in Figure 7.

Nahcolite in natural fluid inclusions

Beyond its appearance in the evaporite ore deposits, nahcolite has been found as a daughter mineral in fluid inclusions in rocks of magmatic origin; e.g., ijolite pegmatites (Rankin and Le Bas, 1974; Aspden, 1980), phonolites (Vard and Williams-Jones, 1993), carbonatites (Rankin, 1977; Samson et al., 1995) and basaltic glasses (Kamenetsky et al., 2001, 2002). It also has been discovered as a daughter mineral in some fluid inclusions in rocks of metamorphic origin; e.g., schists (Ram Mohan and Prasad, 2002), eclogites (Andersen et al., 1989), granulites (Larsen et al., 1998), greenstones (Samson et al., 1997), migmatites (Olsen, 1987), and alkaline metasomatic alteration zones between basic-ultrabasic rocks and pegmatites (Moroz et al., 2001; Vapnik and Moroz, 2002). In general nahcolite has been considered to be part of the crystallization products of these fluid inclusions at low tempera-

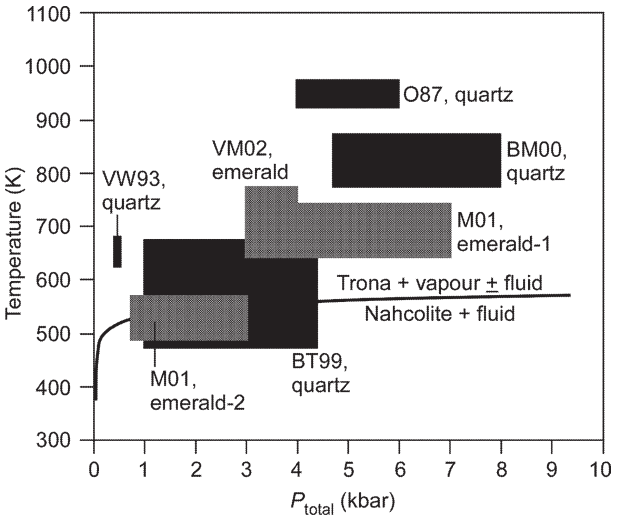

Figure 8. *P–T* conditions of natural fluid inclusions hosting nahcolite. The univariant curve of nahcolite + trona + vapour + fluid determined in Fig. 6 is also sketched ($pCO_2 \approx P_{total}$). Fluid inclusions hosting nahcolite grains occur in quartz or emerald. O87, Olsen (1987); VW93, Vard and Williams-Jones (1993); BT99, Barrie and Touret (1999); BM00, Bakker and Mamtani (2000); M01, Moroz et al. (2001); VM02, Vapnik and Moroz (2002). Emerald-1 in Moroz et al. (2001) was from the Lake Manyara deposit whereas Emerald-2 was from the Sumbawanga deposit of Tanzania.

tures. On the other hand, nahcolite in the fluid inclusions in the quartz grains from a biotite-garnet schist in the Southern Aravalli Mountain Belt (Bakker and Mamtani, 2000) and some auriferous veins at Yirisen, Masumbiri, Sierra Leone (Barrie and Touret, 1999) has been interpreted as an accidentally trapped mineral. Due to the lack of experimental data on the physical-chemical behavior of nahcolite at moderate-to-high pressures, the actual mechanism by which nahcolite formed in these fluid inclusions was uncertain.

The trapping *P–T* conditions of some fluid inclusions which host nahcolite are plotted in Figure 8. These trapping *P–T* conditions were established by microthermometry (Barrie and Touret, 1999; Bakker and Mamtani, 2000; Moroz et al., 2001; Vapnik and Moroz, 2002), mineralogical geothermometry-geobarometry (Olsen, 1987) or stratigraphic reconstruction combined with fluid inclusion isochors (Vard and Williams-Jones, 1993). According to our experimentally determined univariant curve of nahcolite + trona + vapour + fluid, the mostly likely stable sodium carbonate-sodium hydrogen carbonate phase in these fluid inclusions at the trapping *P–T* conditions appears to be trona rather than nahcolite, and any nahcolite grains accidentally trapped by the fluids in excess (Barrie and Touret, 1999; Bakker and Mamtani, 2000) probably would be dissolved in the fluids due to the high temperature. Indeed trona has been occasionally documented in the field (Markl and Baumgartner, 2002). Consequently it should be concluded that nahcolite in these natural occurrences is most likely a daughter mineral which crystallized from the fluids as temperature decreased.

ACKNOWLEDGMENTS

We thank K.R. Law and G.C. Yau for their help with the XRD analyses. This work was supported by a Discovery Grant from the Natural Sciences and Engineering Research Council of Canada.

REFERENCES

Andersen, T., Burke, E.A.J. and Austrheim, H. (1989) Nitrogen-bearing, aqueous fluid inclusions in some eclogites from the Western Gneiss Region of the Norwegian Caledonides. Contributions to Mineralogy and Petrology, 103, 153-165.

Aspden, J.A. (1980) The mineralogy of primary inclusions in apatite crystals extracted from Alnö ijolite. Lithos, 13, 263-268.

Bakker, R.J. and Mamtani, M.A. (2000) Fluid inclusions as metamorphic process indicators in the Southern Aravalli Mountain Belt (India). Contributions to Mineralogy and Petrology, 139, 163-179.

Barrie, I.J. and Touret, J.L.R. (1999) Fluid inclusion studies of gold-bearing quartz veins from the Yirisen deposit, Sula Mountains greenstone belt, Masumbiri, Sierra Leone. Ore Geology Reviews, 14, 203-225.

Bohlen, S.R. (1984) Equilibria for precise pressure calibration and a frictionless furnace assembly for the piston-cylinder apparatus. Neues Jahrbuch füer Mineralogie, Monatshefte, 404-412.

Caven, R.M. and Sand, H.J.S. (1911) The dissociation pressures of alkali bicarbonates. Part I. Sodium hydrogen carbonate. Journal of the Chemical Society, Transactions, 99, 1359-1369.

Chrastil, J. (1982) Solubility of solids and liquids in supercritical gases. Journal of Physical Chemistry, 86, 3016-3021.

Dawson, J.B. (1962) Sodium carbonate lavas from Oldoinyo Lengai, Tanganyika. Nature, 195, 1076-1077.

Dei, L. and Guarini, G.G.T. (1997) The thermal decomposition of $NaHCO_3$: renewed studies by DSC, SEM and FT-IR. Journal of Thermal Analysis, 50, 773-783.

Duan, Z. and Sun, R. (2003) An improved model calculating CO_2 solubility in pure water and aqueous NaCl solutions from 273 to 533 K and from 0 to 2000 bar. Chemical Geology, 193, 257-271.

Duan, Z., Møller, N. and Weare, J.H. (1995) Equation of state for the $NaCl-H_2O-CO_2$ system: Prediction of phase equilibria and volumetric properties. Geochimica et Cosmochimica Acta, 59, 2869-2882.

Duan, Z., Møller, N. and Weare, J.H. (1992) An equation of state for the $CH_4-CO_2-H_2O$ system: II. Mixtures from 50 to 1000 °C and 0 to 1000 bar. Geochimica et Cosmochimica Acta, 56, 2619-2631.

Dyni, J.R. (1996) Sodium carbonate resources of the Green River Formation. U.S. Geological Survey Open-File Report, 96-729.

Eugster, H.P. (1966) Sodium carbonate-bicarbonate minerals as indicators of pCO_2. Journal of Geophysical Research, 71, 3369–3377.

Foshag, W.F. (1940) Sodium bicarbonate (nahcolite) from Searles Lake, California. American Mineralogist, 25, 769–778.

Freeth, F.A. (1923) The system Na_2O–CO_2–NaCl–H_2O, considered as two four-component systems. Philosophical Transactions of the Royal Society of London, A223, 35–87.

Gancy, A.B. (1963) Thermal decomposition of sodium sesquicarbonate. Journal of Chemical & Engineering Data, 8, 301–306.

Hendel, E. M. and Hollister, L.S. (1981) An empirical solvus for CO_2–H_2O–2.6 wt% salt. Geochimica et Cosmochimica Acta, 45, 225–228.

Hill, A.E. and Bacon, L.R. (1927) Ternary systems. VI. Sodium carbonate, sodium bicarbonate and water. Journal of the American Chemical Society, 49, 2487–2495.

Kagi, H., Nagai, T., Komatsu, K., Okada, T., Wada, C., Loveday, J.S. and Parise, J.B. (2005) Pressure response on hydrogen bonds in potassium hydrogen carbonate and sodium hydrogen carbonate. Journal of Neutron Research, 13, 21–26.

Kamenetsky, V.S., Binns, R.A., Gemmell, J.B., Crawford, A.J., Mernagh, T.P., Maas, R. and Steele, D. (2001) Parental basaltic melts and fluids in eastern Manus backarc Basin: implications for hydrothermal mineralisation. Earth and Planetary Science Letters, 184, 682–702.

Kamenetsky, V.S., Davidson, P., Mernagh, T.P., Crawford, A.J., Gemmell, J.B., Portnyagin, M.V. and Shinjo, R. (2002) Fluid bubbles in melt inclusions and pillow-rim glasses: high-temperature precursors to hydrothermal fluids? Chemical Geology, 183, 349–364.

Keller, J. and Krafft, M. (1990) Effusive natrocarbonatite activity of Oldoinyo Lengai, June 1988. Bulletin Volcanologie, 52, 629–645.

Larsen, R.B., Eide, E.A. and Burke, E.A.J. (1998) Evolution of metamorphic volatiles during exhumation of microdiamond-bearing granulites in the Western Gneiss Region, Norway. Contributions to Mineralogy and Petrology, 133, 106–121.

Lowe, D.R. and Tice, M.M. (2004) Geologic evidence for Archean atmospheric and climatic evolution: fluctuating levels of CO_2, CH_4, and O_2 with an overriding tectonic control. Geology, 32, 493–496.

Lowenstein, T.K. and Demicco, R. V. (2006) Elevated Eocene atmospheric CO_2 and its subsequent decline. Science, 313, 1928.

Markl, G. and Baumgartner, L. (2002) pH changes in peralkaline late-magmatic fluids. Contributions to Mineralogy and Petrology, 144, 331–346.

Mees, F., Reyes, E. and Keppens, E. (1998) Stable isotope chemistry of gaylussite and nahcolite from the deposits of the crater lake at Malha, northern Sudan. Chemical Geology, 146, 87–98.

Mirwald, P.W., Getting, I.C. and Kennedy, G.C. (1975) Low-friction cell for piston-cylinder high-pressure apparatus. Journal of Geophysical Research, 80, 1519–1525.

Monnin, C. and Schott, J. (1984) Determination of the solubility products of sodium carbonate minerals and an application to trona deposition in Lake Magadi (Kenya). Geochimica et Cosmochimica Acta, 48, 571–581.

Moroz, I., Vapnik, Y., Eliezri, I. and Roth, M. (2001) Mineral and fluid inclusion study of emeralds from the Lake Manyara and Sumbawanga deposits, Tanzania. Journal of Africa Earth Sciences, 33, 377–390.

Olsen, S.N. (1987) The composition and role of fluid in migmatites: a fluid inclusion study of the Front Range rocks. Contributions to Mineralogy and Petrology, 96, 104–120.

Pitzer, K.S. (1973) Thermodynamics of electrolytes. I. Theoretical basis and general equations. Journal of Physical Chemistry, 77, 268–277.

Ram Mohan, M. and Prasad, P.S.R. (2002) FTIR investigation on the fluid inclusions in quartz veins of the Penakacherla Schist Belt. Current Science, 83, 755–760.

Rankin, A.H. (1977) Fluid-inclusion evidence for the formation conditions of apatite from the Tororo carbonatite complex of eastern Uganda. Mineralogical Magazine, 41, 155–164.

Rankin, A.H. and Le Bas, M.J. (1974) Nahcolite ($NaHCO_3$) in inclusions in apatites from some E. African ijolites and carbonatites. Mineralogical Magazine, 39, 564–570.

Robie, R.A. and Hemingway, B.S. (1995) Thermodynamic properties of minerals and related substances at 298.15 K and 1 bar (10^5 pascals) pressure and at higher temperatures. U.S. Geological Survey Bulletin, 2131.

Rupert, J.P., Hopkins, H.P. and Wulff, C.A. (1965) The solution thermochemistry of polyvalent electrolytes. IV. Sodium carbonate, sodium bicarbonate, and trona. The Journal of Physical Chemistry, 69, 3059–3062.

Samson, I.M., Liu, W. and Williams-Jones, A.E. (1995) The nature of orthomagmatic hydrothermal fluids in the Oka carbonatite, Quebec, Canada: evidence from fluid inclusions. Geochimica et Cosmochimica Acta, 59, 1963–1977.

Samson, I.M., Bas, B. and Holm, P.E. (1997) Hydrothermal evolution of auriferous shear zones, Wawa, Ontario. Economic Geology, 92, 325–342.

Sterner, S.M. and Bodnar, R.J. (1991) Synthetic fluid inclusions; X, Experimental determination of P-V-T-X properties in the CO_2–H_2O system to 6 kb and 700 °C. American Journal of Science, 291, 1–51.

Sugitani, K., Mimura, K., Suzuki, K., Nagamine, K. and Sugisaki, R. (2003) Stratigraphy and sedimentary petrology of an Archean volcanic-sedimentary succession at Mt. Goldsworthy in the Pilbara Block, Western Australia: implications of evaporite (nahcolite) and barite deposition. Precambrian Research, 120, 55–79.

Templeton, C.C. (1978) Pressure-temperature relationship for decomposition of sodium bicarbonate from 200 to 600°F. Journal of Chemical & Engineering Data, 23, 7–11.

Vanderzee, C.E. (1982) Thermodynamic relations and equilibria in (Na_2CO_3 + $NaHCO_3$ + H_2O): standard Gibbs energies of formation and other properties of sodium hydrogen carbonate, sodium carbonate heptahydrate, sodium carbonate decahydrate, trona: (Na_2CO_3·$NaHCO_3$·$2H_2O$), and Wegscheider's salt: (Na_2CO_3·$3NaHCO_3$). The Journal of Chemical Thermodynamics, 14, 219–238.

Vapnik, Y. and Moroz, I. (2002) Compositions and formation conditions of fluid inclusions in emerald from the Maria deposit (Mozambique). Mineralogical Magazine, 66, 201–213.

Vard, E. and Williams-Jones, A.E. (1993) A fluid inclusion study of vug minerals in dawsonite-altered phonolite sills, Montreal, Quebec: implications for HFSE mobility. Contributions to Mineralogy and Petrology, 113, 410–423.

Waldeck, W.F., Lynn, G. and Hill, A.E. (1934) Aqueous solubility of salts at high temperatures. II. The ternary system Na_2CO_3–$NaHCO_3$–H_2O from 100° to 200°. Journal of the American Chemical Society, 56, 43–47.

Wang, J., Zhang, Y., Yang, Q., Zhou, J. and Ma, X. (1991) The

geological characteristics and origin of the Anpeng alkali deposit. Geological Review, 37, 42–50.

Wiebe, R. and Gaddy, V.L. (1939) The solubility in water of carbon dioxide at 50, 75 and 100°, at pressures to 700 atmospheres. Journal of the American Chemical Society, 61, 315–318.

Zaitsev, A.N. and Keller, J. (2006) Mineralogical and chemical transformation of Oldoinyo Lengai natrocarbonatites, Tanzania. Lithos, 91, 191–207.

Manuscript received April 2, 2008
Manuscript accepted August 26, 2008

Manuscript handled by Masaki Enami